

ChemComm

Accepted Manuscript



This is an *Accepted Manuscript*, which has been through the Royal Society of Chemistry peer review process and has been accepted for publication.

Accepted Manuscripts are published online shortly after acceptance, before technical editing, formatting and proof reading. Using this free service, authors can make their results available to the community, in citable form, before we publish the edited article. We will replace this *Accepted Manuscript* with the edited and formatted *Advance Article* as soon as it is available.

You can find more information about *Accepted Manuscripts* in the [Information for Authors](#).

Please note that technical editing may introduce minor changes to the text and/or graphics, which may alter content. The journal's standard [Terms & Conditions](#) and the [Ethical guidelines](#) still apply. In no event shall the Royal Society of Chemistry be held responsible for any errors or omissions in this *Accepted Manuscript* or any consequences arising from the use of any information it contains.

COMMUNICATION

Platinum Decorated Functionalized Defective Acetylene Black; A Promising Cathode Material For Oxygen Reduction Reaction

Cite this: DOI: 10.1039/x0xx00000x

Received 00th January 2012,
Accepted 00th January 2012

B. Rajashekar, R. Vedarajan and N. Matsumi

DOI: 10.1039/x0xx00000x

www.rsc.org/

A novel single-pot method to exfoliate and functionalize acetylene black was proposed. The deliberate functionalization was found to enhance the intrinsic oxygen reduction efficiency along with nucleation and growth of platinum nano-particles on the surface. The resultant material showed enormously high oxygen reduction reactivity compared to its commercial counterparts.

The global scenario of energy depletion has led to an aggressive outlook for different electrochemical devices and in particular for the ones that uses renewable energy. The applications of different types of carbon to electrochemical devices, especially in the field of energy viz., fuel cells and Li-air battery are of significance currently, as they project high energy density with prolonged durability. The major limiting factor that affects the efficiency of these devices is the sluggishness of the Oxygen Reduction Reaction (ORR) at the cathode. Hence, the need for an efficient cathode material has been under continuous research. The advancement in the field of material science and nano-technology has led to the discovery of many novel carbon material in varied dimensional orders such as Fullerene, CNT, graphene, carbon blacks etc as an effective support for ORR. The attributes looked for an efficient ORR material of choice should possess high surface area of carbon support, ability to support the catalyst, high pore size, negligible charge transfer resistance and high cyclability of carbon^{1,2}. All the aforementioned properties also affect the kinetics of cathode reaction. Graphite which is currently used in many commercially available electrochemical devices suffers from properties like low surface area and high charge transfer resistance. Among all the carbon materials, the magical material, 'graphene' over powers all the other carbon material for many applications. But, unfortunately its arduous preparation methods hinder its commercialization. Hence, in order to reap the benefits of the high energy density devices, the need for novel carbon material with enhanced inherent properties is the need of the hour.

Recently researchers have started to revisit acetylene black (AB) as carbon support for various applications^{3,4}. In past Uchida et al.^{5,6} showed tremendous activity of AB as carbon support for proton exchange membrane fuel cells and direct-methanol fuel cells. Generally graphite is used as cathode material along with carbon black such as acetylene black (AB) as binder. Though graphite has better conductivity, acetylene black (AB) can override graphite as it has properties such as i) low resistivity in the presence of electrolyte and an active electrode material by itself, ii) absorb and retain significant volume of electrolyte without reducing its capability of mixing with the active material iii) high surface area and iv) economical compared to its counterparts. AB can become a prospective material for use as active electrode material by tuning inherent properties of AB. However AB's concern regarding cyclability cannot be overlooked. Preliminary experiments by us indicated enormous potential in AB as an efficient cathode material. Hence, it was conceded that by modifying the surface of AB with a facile procedure to enhance its ability to support the catalyst, reduction of charge transfer resistance, increasing its surface area by exfoliating its graphitic layers and increasing its durability would epitomize the attributes of AB. In this work, we present a simple methodology to make a unique functionalized carbon material. This work also demonstrates the importance of functionalization or defects on to the surface of AB in order to attain a well dispersed nucleation of Pt over AB. This functionalization not only led to an improvement in the overall distribution of Pt-nanoparticles (Pt-np) impregnated over the surface of AB but also, thus, decorated Pt-nanoparticles formed a protective shield against the easy degradation of AB.

Acetylene black was functionalized and exfoliated using a facile single pot method. Firstly, AB was mixed with 3:1 H₂SO₄: HNO₃ and ultrasonicated for 3 hrs to get exfoliated and functionalized acetylene black (FAB). The functionalized acetylene black was

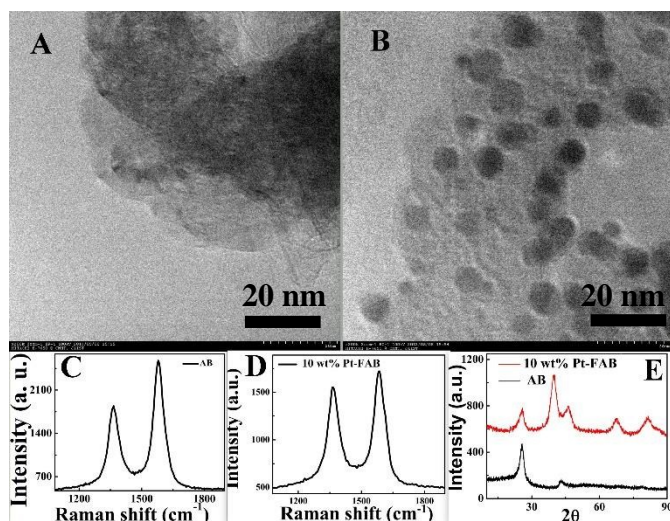


Fig. 1 (A, B) TEM micrographs of AB and Pt-FAB, (C, D) Raman spectra of AB and 10 wt% Pt-FAB and (E) XRD of AB and 10 wt% Pt-FAB.

further decorated with Pt-nano particles (Pt-np) using standard reduction procedure using H₂PtCl₆ in ethylene glycol⁷. The reduction procedure resulted in a uniform distribution of Pt-nps over the surface of FAB. The loading of Pt was carried out under Pt amount of 8, 10 and 40 wt%. As-prepared Pt-FAB was characterized with the help of transmission electron microscopy, Raman spectroscopy, XPS and X-ray diffraction techniques. Along with these, catalytic efficiency, charge transfer resistance and durability of the material were characterized using electrochemical techniques like cyclic voltammetry and electrochemical impedance spectroscopy.

The TEM analyses of AB and Pt-FABs shed light on the dispersivity of the nano particles, particle size distribution and the exfoliation characteristics of the AB. Unlike the multi-layered and interconnected morphology of untreated AB (Fig.1A), Pt-FAB (Fig.1B) exhibited a well dispersed, graphene-like transparent feature. Further, the Pt-np were found to be uniformly studded all through the surface of FAB in concentric circles which can be attributed to the circular grains of AB⁸. The grain boundaries being predominately activated compared to the bulk of the grain might be the reason for such an observation. This was not a localized but an average phenomenon, noted in all the batches of synthesis. The average size of the Pt particles were in the range of 3 – 6 nm. Energy dispersive X-ray spectroscopy (EDS) (Fig.ESI 4) confirmed the incorporation of Pt on FAB and the amount of Pt present in each sample was determined to be 10% in weight (10 wt%). Raman analysis of AB and 10 wt% Pt-FAB exhibited a typical spectrum for carbonaceous material. A blue shift of 5 cm⁻¹ was observed in the D-band of 10 wt% Pt-FAB compared to AB. Further an increase in the Id/Ig ratio and in the full width half maxima (FWHM) for D band at 64.0cm⁻¹ for AB to 69.5cm⁻¹ for 10 wt% Pt-FAB confirms the increase in defects which can be attributed to the deliberate oxidation of the carbon material⁹. X-ray photo electron spectroscopic (XPS) characterization confirmed the deliberate oxidation of the surface of AB to form FAB. Comparison of the wide region spectral survey showed an increase in the amount of oxygen from 2% in AB to around 10% in FAB. Deconvolution of C(1s) peak revealed the formation of –COOH groups on the surface of FAB. As shown in Fig (ESI 1), FAB consist of following types of carbons; C (284.6 eV), C–OH bonds (285.1 eV), carbonyl C(C=O, 286.0 eV), and carboxylate carbon (O–C=O, 286.7 eV).

X-ray powder diffraction (XRD) technique was used for studying the crystallinity of carbon and Pt-nps. Fig.1E shows the XRD diffraction pattern of AB and 10 wt %Pt-FAB. The diffractogram of AB is featured by two typical peaks at 2θ values of 25.70 and 43.00 corresponding to (002) and (100), respectively. Diffraction pattern for the Pt-FAB showed strong peaks at 2θ values of 39.60, 46.20, 67.60, and 81.40 which corresponds to Pt (111), (200), (220) and (311), respectively. The presence of the crystalline planes of face-centred-cube (fcc) structure evince the decoration of crystalline Pt-nps. The average particle size of the spherical Pt-nps (as seen in TEM) was calculated using the Sherrer's equation: $D = 0.89\lambda / (B \cos \theta)$ where, $\lambda = 0.154$ nm and B is the full width at half-maximum (FWHM) of diffraction pattern of Pt (220)⁷. The calculated average particle size was 3.09 nm which is in concordance with the average size range estimated from TEM measurements.

Electrocatalytic ORR activity and Electrochemical Surface Area (ECSA) of AB, FAB and Pt-FAB were evaluated using cyclic voltammetry (CV) technique. CV measurements were carried out in nitrogen saturated 0.1M HClO₄ (aq.) using Pt wire as counter electrode, glassy carbon electrode coated with thin-film of materials under study (ink preparation was carried out as detailed in ESI) as working electrode. All the experiments were carried out at a potential scan rate of 20 mVs⁻¹ (Ag/AgCl). Fig. 2 shows the cyclic voltammogram of 10 wt% Pt-FAB in comparison with 20 wt%Pt-Vulcan XC-72 (purchased from sigma aldrich). The voltammograms exhibits the electrochemical fingerprints of Pt in the electrode. It shows the typical peaks of H₂ adsorption and desorption at -0.2 V, H₂ desorption spillover at -0.05 V, oxygen evolution at 0.43 V and ORR at 0.44 V (vs Ag/AgCl). The ECSA was determined using desorption peak from the CV (equation provided in ESI) ECSA for 10 wt% Pt-FAB was found to be approximately 35 m²/g while that of 20 wt% Pt-Vulcan XC-72 was found to be 30.6 m²/g. This can be attributed to the smaller average particle size of 10 wt% Pt-FAB which was determined to be <5 nm and while that for Pt/C was observed to be >5 nm. These voltammogram results apparently indicated the better performance by 10 wt% Pt-FAB compared to commercial 20 wt%Pt-Vulcan XC-72.

Inset of Fig. 2 shows the cyclic voltammograms of AB and FAB which are noteworthy, because of their impressive ORR activity even without any metal loading. Many researchers have

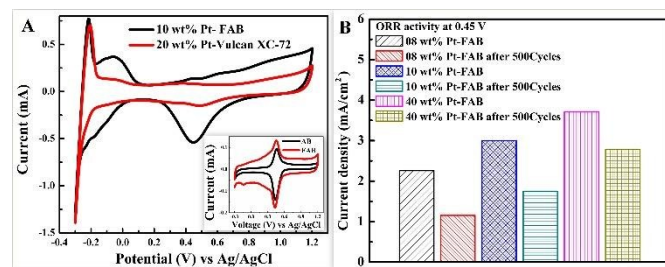


Fig. 2 A) Voltammograms of 10wt% Pt-FAB in comparison with 20wt% Pt-Vulcan XC-72. Inset shows the voltammograms of AB and FAB. B) Shows the durability of Pt-FABs in terms of ORR current after 500th cycle

shown in past that the presence of hetero atom which creates partial charge on the carbon atoms can perform ORR and OER even without any catalytic metal atoms^{10,11}. As the oxygen functionalities increases, the ORR activity also increases, this can be unmistakably confirmed by the intensity of the ORR current in cyclic voltammetry. Oxygen functionalities not only act as the active sites for ORR but also plays a major role as nucleation sites and

anchoring sites¹² for the formation of metal-nps. The effect due to the presence of functional groups can be appreciated by comparing the TEM images of Pt decorated AB (Fig ESI 2) and FAB (Fig. 1B). The main differences between AB and FAB are i) an increased double layer capacitance; can be attributed to the exfoliation leading to higher surface area which in turn leads to higher double layer capacitance as observed from the region 0.2 – 0.4V in the voltammogram ii) increase in ORR peak intensity of FAB; an apparent increase in the ORR current of FAB was observed compared to AB. The current increased from 0.139 mA of the later

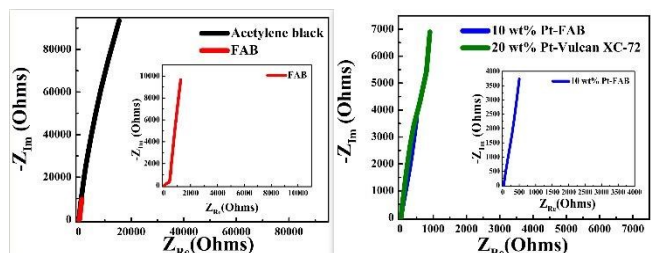


Fig. 3 The Nyquist plot of A) AB and FAB B) 10 wt% Pt-FAB and 20 wt% Pt-Vulcan XC-72

to 0.177 mA for FAB. Also a significant shift in onset potential was observed.

One of the attractive aspect of AB which makes it an efficient cathode material is its interaction with electrolyte i.e., its ability to absorb and retain significant volume of electrolyte. Interaction with electrolyte influences in reducing the interface boundaries which in turn effects the overall catalytic performance of the electrode^{13,14}. Hence, interfacial studies are vital to validate the catalytic performance of electrode, which can be understood by electrochemical impedance studies. The electrochemical impedance spectroscopy results presented in the Fig. 3 exhibited typical spectra of such ORR catalysts¹⁵. However fitting with an equivalent circuit (Fig ESI 5) revealed a unique behaviour unlike conventional Pt/C catalyst. In addition to the charge transfer realized at the Pt/C interface, two additional elements contributed to the impedance. Due to the high absorptivity of AB, a double layer formed at the interface of glassy carbon can be classed into two elements. One of these elements can be attributed to the electrolyte absorption over AB layer (R4), the other one can be attributed to the direct influence of the electrolyte on the surface of the GC (R3). R_{sol} represents the resistance of the electrolyte and χ^2 is the error of the theoretical fitting. Schematic representation explaining all the elements are shown in ESI 6a-b. Table 1 shows charge transfer resistance (R_{CT}) values along with other elements of the equivalent circuit of all the 4 AB related material in comparison with 20wt%Pt-Vulcan XC-72.

	AB	FAB	10% Pt-FAB	40% Pt-FAB	20%Pt-Vulcan XC-72
R _{sol} (Ω)	41.66	38.11	52.94	31.55	31.65
R _{CT} (Ω)	37.89	33.99	22.82	20.10	378.80
R3(Ω)	96.38	454.90	2408.00	3359.00	5.62E4
R4(Ω)	4.19E5	7.01E4	2.087E4	6.962E4	
χ^2	10 ⁻⁴	10 ⁻⁴	10 ⁻⁴	10 ⁻⁵	10 ⁻⁴

Table 1: Comparison of elements in the equivalent circuits along with R_{CT}

Further, the durability of the material was investigated by subjecting the materials to 500 cycles of potential scan from -0.3V to 1.2V vs Ag/AgCl electrode. It was observed that the cyclability of the material had substantially increased through Pt-np decoration on to the FAB. The charge-density at 0.44V was studied before and after 500 cycles. The charge density for 8 wt% Pt-FAB was reduced from 2.26 mA/cm² to 1.15 mA/cm², 10 wt% Pt-FAB from 3.00 mA/cm² to 1.75 mA/cm² and 40 wt% Pt-FAB from 3.7 mA/cm² to 2.7 mA/cm² before and after 500 potential cycles. It was also observed that the durability is in the order of amount of Pt-np decoration. Fig. 2B shows the cyclability of 8, 10 and 40 wt% of Pt-FAB. By increasing the Pt loading amount from 8 to 40 wt%, the cyclability increased by nearly 25%. Durability test for Pt-FAB and commercial Pt/C was also conducted and found that charge density of 20 wt% Pt-Vulcan XC-72 is only 0.71 mA/cm². When compared with this, Pt-FAB has found to show 60% more ability in reducing the oxygen even after 100 potential scans (Fig ESI 3).

Conclusions

A novel disordered graphene like material was prepared using AB as starting material with a facile single pot method which can be easily scaled up. Upon surface modification with Pt-np decoration, it showed an enormous catalytic activity when compared to commercial Pt/C. The reasons for the above activity was evaluated to be having high electrochemical surface area, low charge transfer resistance and disorders on the surface. Above results and observations showed that Pt-FAB is a promising ORR catalyst which can find its application in fuel cell and metal air batteries.

Notes and references

^a School of Materials Science, Japan Advanced Institute of Science and Technology, Nomi, Ishikawa 923-1292, Japan.

Electronic Supplementary Information (ESI) available. See DOI: 10.1039/c000000x/

- 1 M. Park, H. Sun, H. Lee, J. Lee and J. Cho, *Adv. Energy Mater.*, 2012, **2**, 780–800.
- 2 J. Xiao, D. Wang, W. Xu, D. Wang, R. E. Williford, J. Liu and J.-G. Zhang, *J. Electrochem. Soc.*, 2010, **157**, A487–A492.
- 3 B. Zhang, C. Lai, Z. Zhou and X. P. Gao, *Electrochim. Acta*, 2009, **54**, 3708–3713.
- 4 H. C. Shin, W. I. Cho and H. Jang, *Electrochim. Acta*, 2006, **52**, 1472–1476.
- 5 M. Uchida, Y. Fukuoka, Y. Sugawara, H. Ohara and A. Ohta, *J. Electrochem. Soc.*, 1998, **145**, 3708–3713.
- 6 M. Uchida, Y. Aoyama, M. Tanabe, N. Yanagihara, N. Eda and A. Ohta, *J. Electrochem. Soc.*, 1995, **142**, 2572–2576.
- 7 Y. Li, W. Gao, L. Ci, C. Wang, and P. M. Ajayan, *Carbon*, 2010, **48**, 1124–1130.
- 8 M. Wissler, *J. Power Sources*, 2006, **156**, 142–150.
- 9 A. C. Ferrari and J. Robertson, *Phys. Rev. B*, 2000, **61**, 14095–14107.
- 10 S. Wang, E. Iyyamperumal, A. Roy, Y. Xue, D. Yu and L. Dai, *Angew. Chem. Int. Ed.*, 2011, **50**, 11756–11760.
- 11 L. Yang, S. Jiang, Y. Zhao, L. Zhu, S. Chen, X. Wang, Q. Wu, J. Ma, Y. Ma and Z. Hu, *Angew. Chem.*, 2011, **123**, 7270–7273.
- 12 Y.-G. Zhou, J.-J. Chen, F. Wang, Z.-H. Sheng and X.-H. Xia, *Chem. Commun.*, 2010, **46**, 5951–5953.
- 13 M. Kim, J.-N. Park, H. Kim, S. Song and W.-H. Lee, *J. Power Sources*, 2006, **163**, 93–97.
- 14 F. Cai, J. Liang, Z. Tao, J. Chen and R. Xu, *J. Power Sources*, 2008, **177**, 631–636.
- 15 A. S. Bondarenko, I. E. L. Stephens, H. A. Hansen, F. J. Pérez-Alonso, V. Tripkovic, T. P. Johansson, J. Rossmeisl, J. K. Nørskov and I. Chorkendorff, *Langmuir*, 2011, **27**, 2058–2066.